3D VTI traveltime tomography for near-surface imaging

Lina Zhang, Jie Zhang, Wei Zhang, University of Science and Technology of China (USTC)*

Summary

Seismic first arrivals that propagate in the near surface area are affected by velocity anisotropy. With VTI assumption for the media, we develop a grid-based qP wave traveltime tomography method to invert Thomsen parameters, including ε and δ at each grid point in the shallow area. In numerical experiments, we fix the symmetry axis velocity V_{p0}, inverting only ε and δ. For single-parameter inversion, we invert ε and δ respectively, and for two-parameter inversion, we invert ε and δ simultaneously. Results indicate that ε is better resolved than δ from inverting the first arrivals.

Introduction

The study of seismic anisotropy has dramatically increased over the past two decades because of advances in parameter estimation, the transition from post-stack imaging to prestack depth migration, the wider offset and better azimuthally coverage of 3D seismic surveys, and acquisition of high-quality multi-component data. Anisotropic effects have become increasingly important in seismic exploration. A detailed historical analysis of developments in seismic anisotropy can be found in Helbig and Thomsen (2005), Tsvankin et al. (2010).

In recent years, many methods for estimating anisotropy parameters in the deep subsurface media have been developed in reflection seismology. Tsvankin and Thomsen (1995), Alkhalifah and Tsvankin (1995), and Grechka and Tsvankin (1998) analyze NMO moveout and invert velocity and η in time domain, the parameter η is defined by ε and δ. Koren et al. (2008) develop a local tomography method that estimates δ from short offset events and ε from long offset data. Schleicher et al. (2010), Huang et al. (2007), Bowling et al. (2009) and Bakulin et al. (2010a, 2010b) develop single-parameter tomography. Zhou et al. (2003) proposes a 3D reflection traveltime tomography that simultaneously inverts for the anisotropy parameters. Jiang et al. (2009) develop a 2D TTI media traveltime tomography for crosshole and VSP geometry.

Near-surface anisotropy, however, has been ignored in seismic studies. Zhang et al. (2012) demonstrate that even weak anisotropy in the near surface area could produce significant artifacts if assuming isotropic in traveltime inversion. In this study, we present a 3D traveltime tomography method for inverting single or multiple anisotropic parameters in the near surface area.

Velocity equation

In anisotropic media, phase velocity and group velocity are different, the phase velocity can be obtained directly from the Christoffel equation, and the group velocity can be obtained only from phase velocity. We adopt the shortest path raytracing method (Zhou and Greenhalgh 2005; Bai et al., 2007) to expand the wavefront using an approximate group velocity (Fomel, 2004) of the VTI media:

$$\frac{1}{V_g^2(\varphi)} = \frac{1+2Q}{2(1+Q)}E(\varphi) + \frac{1}{2(1+Q)}\sqrt{E^2(\varphi)+4(Q^2-1)AC\sin^2\varphi\cos^2\varphi}, \\ = \frac{1+2Q}{2(1+Q)}E(\varphi) + \frac{1}{2(1+Q)}D \quad (1)$$

Where φ is the ray angle while

$$Q = 1+2\eta$$
$$A = \frac{1}{V_h^2} = \frac{1}{(1+2\varepsilon)V_{p0}^2}, C = \frac{1}{V_{p0}^2}$$
$$E(\varphi) = A\sin^2\varphi + C\cos^2\varphi,$$
$$D = \sqrt{E^2(\varphi)+4(Q^2-1)AC\sin^2\varphi\cos^2\varphi}$$

Fomel's group velocity approximation is also accurate for strong VTI media (Yuan et al., 2006). An approximate group velocity is frequently used in tomography to derive sensitivity coefficients to the anisotropic parameters (Yuan et al., 2006; Jiang and Zhou, 2011), namely, Frechet derivatives.

Tomography equation

The traveltime of a ray in an anisotropic medium is

$$T = \int_L \frac{1}{V_g} dl \quad (2)$$

Where L is the ray path, and V_g is the group velocity along the ray path. The first order traveltime perturbation is

$$\Delta T = -\int_L \frac{\Delta Vg}{V_g^2} dl \quad (3)$$

The traveltime perturbation with respect to the anisotropic parameters could be written as:

$$\Delta T = \int_L \frac{\partial T}{\partial V_{p0}}\Delta V_{p0} dl + \int_L \frac{\partial T}{\partial \varepsilon}\Delta\varepsilon dl + \int_L \frac{\partial T}{\partial \eta}\Delta\eta dl + \int_L \frac{\partial T}{\partial \theta}\Delta\theta dl + \int_L \frac{\partial T}{\partial \varphi}\Delta\varphi dl \quad (4)$$

The equation (2) can be written as:

$$\mathbf{G(m) = d} \quad (5)$$

Where **m** presents model vector; **d** is traveltime data, where $\mathbf{m} = \left(V_{p0_1}, V_{p0_2}, ..., V_{p0_{Ncell}}, \varepsilon_1, \varepsilon_2, ..., \varepsilon_{Ncell}, \eta_1, \eta_2, ..., \eta_{Ncell}\right)^T$.

DOI http://dx.doi.org/10.1190/segam2013-0915.1

After adding the Tikhonov regularization term, the objective function is defined as:

$$\chi(\mathbf{m})=\frac{1}{2}\left\|\mathbf{d}^{\mathbf{obs}}-\mathbf{G}(\mathbf{m})\right\|^2+\frac{1}{2}\tau_{v_{p0}}\left\|\mathbf{R}_{v_{p0}}\mathbf{m}_{v_{p0}}\right\|^2+\frac{1}{2}\tau_{\varepsilon}\left\|\mathbf{R}_{\varepsilon}\mathbf{m}_{\varepsilon}\right\|^2+\frac{1}{2}\tau_{\eta}\left\|\mathbf{R}_{\eta}\mathbf{m}_{\eta}\right\|^2 \tag{6}$$

Where $\mathbf{R}_{v_{p0}},\mathbf{R}_{\varepsilon},\mathbf{R}_{\eta}$ are regularization operators for the anisotropic parameters, and $\tau_{v_{p0}},\tau_{\varepsilon},\tau_{\eta}$ are corresponding regularization factors.

After dispersing equation (2), equation (6) can be written as:

$$\chi(\mathbf{m})=\frac{1}{2}\sum_{i=1}^{Nl}\left\|\sum_{j=1}^{Ncell}\frac{l_{i,j}}{v_{g_j}(\mathbf{m})}-t_i^{obs}\right\|^2+\frac{1}{2}\tau_{v_{p0}}\left\|\mathbf{R}_{v_{p0}}\mathbf{m}_{v_{p0}}\right\|^2+\frac{1}{2}\tau_{\varepsilon}\left\|\mathbf{R}_{\varepsilon}\mathbf{m}_{\varepsilon}\right\|^2+\frac{1}{2}\tau_{\eta}\left\|\mathbf{R}_{\eta}\mathbf{m}_{\eta}\right\|^2 \tag{7}$$

According to the Gauss-Newton method, equation (7) can be written as:

$$\left[\mathbf{A}^{\mathrm{T}}\mathbf{A}+\tau_{v_{p0}}\mathbf{R}_{v_{p0}}^{\mathrm{T}}\mathbf{R}_{v_{p0}}+\tau_{\varepsilon}\mathbf{R}_{\varepsilon}^{\mathrm{T}}\mathbf{R}_{\varepsilon}+\tau_{\eta}\mathbf{R}_{\eta}^{\mathrm{T}}\mathbf{R}_{\eta}\right]\Delta\mathbf{m}=$$
$$\mathbf{A}^{\mathrm{T}}\left[\mathbf{d}^{\mathbf{obs}}-\mathbf{G}(\mathbf{m})\right]-\tau_{v_{p0}}\left(\mathbf{R}_{v_{p0}}^{\mathrm{T}}\mathbf{R}_{v_{p0}}\mathbf{m}_{v_{p0}}\right)-\tau_{\varepsilon}\left(\mathbf{R}_{\varepsilon}^{\mathrm{T}}\mathbf{R}_{\varepsilon}\mathbf{m}_{\varepsilon}\right)-\tau_{\eta}\left(\mathbf{R}_{\eta}^{\mathrm{T}}\mathbf{R}_{\eta}\mathbf{m}_{\eta}\right)$$
$$\mathbf{A}=\frac{\partial\mathbf{G}}{\partial\mathbf{m}} \tag{8}$$

We use a conjugate gradient method to iteratively solve equation (8) and invert for anisotropic parameters.

Synthetic examples

We use single-parameter and two-parameter methods to invert anisotropy parameters. For single-parameter inversion, we use two different test models and one test model for two-parameter inversion.

Single-parameter inversion

The first test model size is 1km×1km×0.7km. This is a half space model with an anomaly object, the source geometry put on the surface, and the receivers at the bottom of anomaly object. The background velocity is 3000m/s, and the anomaly object is anisotropic.

The anomaly object anisotropic parameters are $V_{p0}=3000m/s,\varepsilon=0.2,\delta=0.15$. After twenty iterations of ε (and δ) updating with fixed the others two parameters, these results are shown on Figure 2 (ε and δ). Figure 1 is the true model section. The misfit curves are displayed on Figure 3. The misfit curves are both convergent, the result of ε (Figure 2a) and δ (Figure 2b) are very similar to the true models (Figure 1). Because the anomaly object locates between sources and receivers, there are more rays through the object, so these inversion results of location and value of anomaly object are very accurate (Figure 2a, 2b).

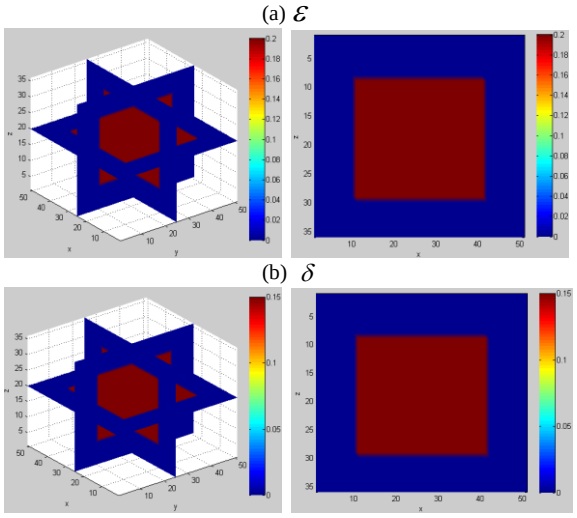

Figure 1: The true 3D VTI model, the left is 3D slice, and the right is vertical slice. (a) ε; (b) δ

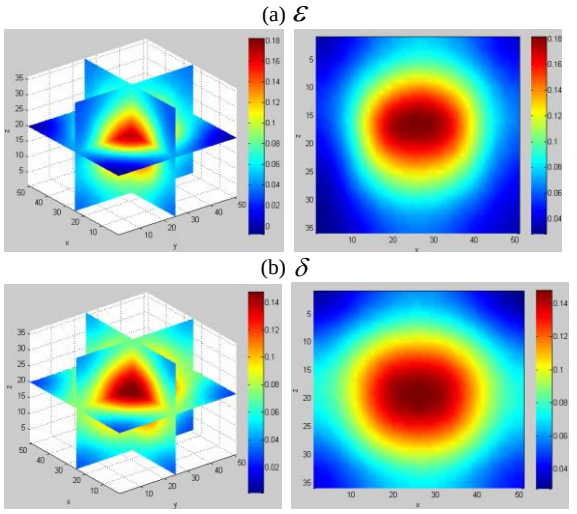

Figure 2: The updated models from the single parameter tomography experiment. The left is 3D slice and the light is vertical slice. (a) ε; (b) δ

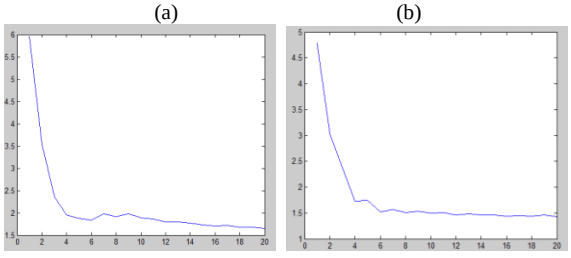

Figure 3: Misfit curves of single parameter inversion. (a) ε; (b) δ

DOI http://dx.doi.org/10.1190/segam2013-0915.1

The second test model size is same as the first, but it is a layer model with an anomaly object. The sources and receivers are put on the surface. The layer model parameters as following (Table 1):

parameter	velocity	thickness
layer_1	2000m/s	100m
layer_2	3000m/s	500m
layer_3	4000m/s	100m

Table 1: The true layer model parameters

And the anomaly object exist in the second layer, these parameters are $V_{p0} = 3000m/s, \varepsilon = 0.2, \delta = 0.15$. The following are the inversion results of ε (Figure 4a) and δ (Figure 4b). Figure 5 is the true model. These inversion results are displayed on Figure 4, and we can see that the result of epsilon is better than delta. Because of the δ influence the traveltime around the symmetry axis and ε determine the traveltime of horizontal direction, when source and receiver geometry are put on the surface, the ray information is more about ε .

(a) ε

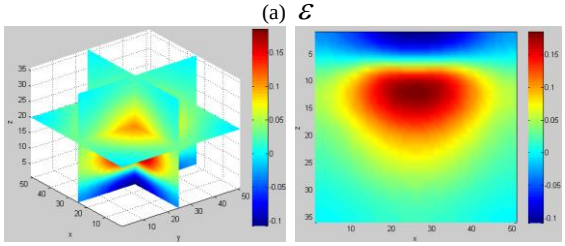

(b) δ

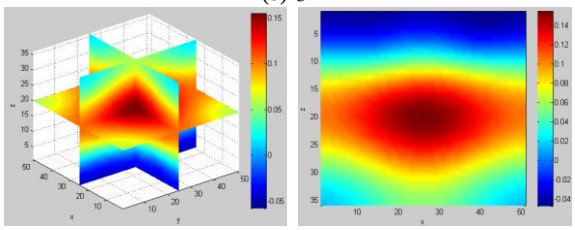

Figure 4: The inversion results of δ and ε , the left is 3D slice, and the right is vertical slice. (a) ε ; (b) δ

(a) ε

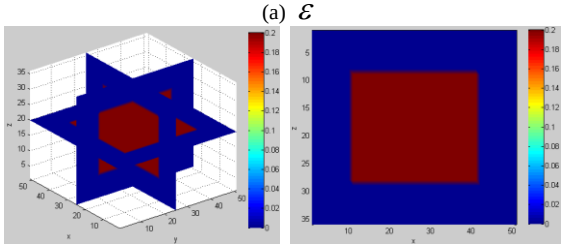

(b) δ

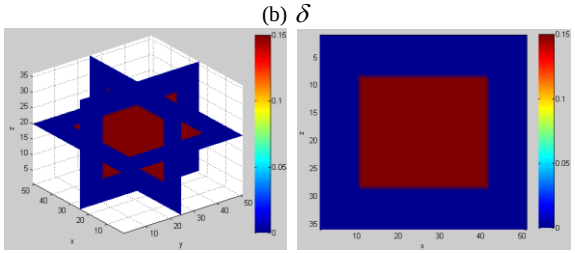

Figure 5: The true 3D model, the left is 3D slice, and the right is vertical slice. (a) ε ; (b) δ .

Multi-parameter inversion

The goal of multi-parameter inversion is to conduct a two-parameter joint tomography that fix the symmetry axis velocity V_{p0} and invert for δ and ε , simultaneously.

This experiment model is a layer model with one layer over half a space, the top layer is anisotropic and the half space is isotropic, the following is the model parameters (Table 2):

parameter	velocity	epsilon	delta	thickness
top layer	2000m/s	0.2	0.15	200m
half space	4000m/s	0.0	0.0	500m

Table 2: The true model parameters of two-parameter inversion

After twenty iterations with fixed symmetry axis velocity V_{p0}, these results are shown on Figure 7, and Figure 6 is the true model.

(a) ε

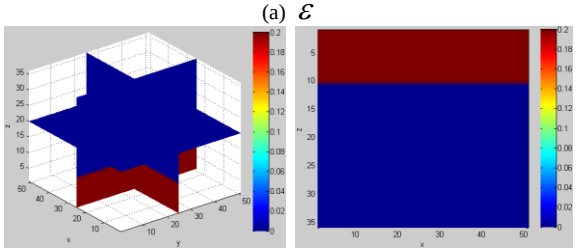

(b) δ

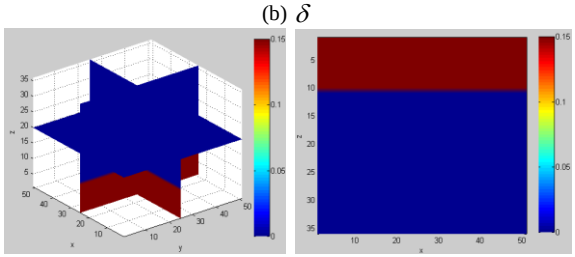

Figure 6: The true 3D model, the left is 3D slice, and the right is vertical slice. (a) ε ; (b) δ .

DOI http://dx.doi.org/10.1190/segam2013-0915.1

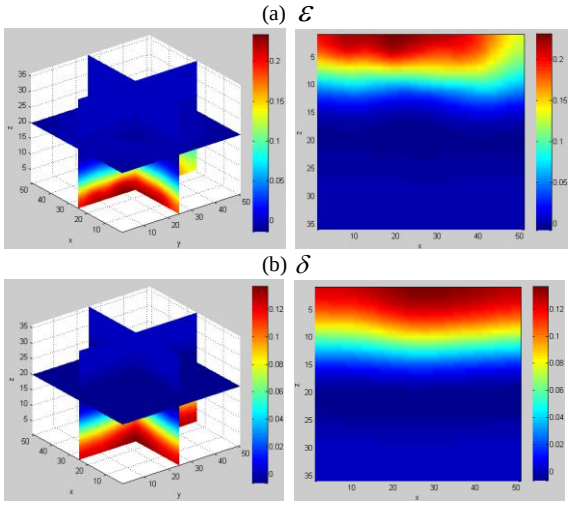

Figure 7: The tomographic result of ε and δ in different direction section. (a) ε; (b) δ.

The inversion results ε and δ are relatively accurate, but there is ambiguity among δ and ε. The inversion value of ε is stronger than the true value, while δ is weaker than the true value. In inversion, the result of δ depends on the initial model, because ε is more sensitive to traveltime, and can be faster to converge to the true model.

Conclusions

We use two methods to implement the VTI traveltime tomography for near surface imaging. For the single-parameter inversion, when traveltimes include more information about ε and δ, we can obtain better results. But in situations, where the source and receiver are put on the surface, ε is more sensitive for traveltime than δ, so the result of ε is more accurate. In theory, two-parameter inversion is a more practical method to invert anisotropy parameters. It can invert δ and ε simultaneously, but there is ambiguity among the anisotropy parameters, and the result of δ depends on the initial model.

Acknowledgements

We appreciate the support from GeoTomo, allowing us to use TomoPlus and VECON software packages to perform this study.

DOI http://dx.doi.org/10.1190/segam2013-0915.1

http://dx.doi.org/10.1190/segam2013-0915.1

EDITED REFERENCES

Note: This reference list is a copy-edited version of the reference list submitted by the author. Reference lists for the 2013 SEG Technical Program Expanded Abstracts have been copy edited so that references provided with the online metadata for each paper will achieve a high degree of linking to cited sources that appear on the Web.

REFERENCES

Alkhalifah, T., and I. Tsvankin, 1995, Velocity analysis in transversely isotropic media : Geophysics, **60**, 1550–1566, http://dx.doi.org/10.1190/1.1443888.

Bai, C., S. Greenhalgh, and B. Zhou, 2007, 3D ray tracing using a modified shortest-path method: Geophysics, **72**, no. 4, T27–T36, http://dx.doi.org/10.1190/1.2732549.

Bakulin, A., Y. Liu, O. Zdraveva, and K. Lyons, 2010b, Anisotropic model building with wells and horizons: Gulf of Mexico case study comparing different approaches: The Leading Edge, **29**, 1450–1460, http://dx.doi.org/10.1190/1.3525359.

Bakulin, A., M. Woodward, D. Nichols, K. Osypov, and O. Zdraveva, 2010a, Building TTI depth models using localized anisotropic tomography with well information: Geophysics, **75**, no. 4, D27–D36, http://dx.doi.org/10.1190/1.3453416.

Bowling, J., S. Ji, D. Lin, M. Reasnor, M. Staines, and N. Burke, 2009, From isotropic to anisotropic: Puma/Mad Dog wide azimuth data case study: 79th Annual International Meeting, SEG, Expanded Abstracts, 246–250, http://dx.doi.org/10.1190/1.3255357.

Fomel, S., 2004, On anelliptic approximations for *qP* velocities in VTI media: Geophysical Prospecting, **52**, 247–259.

Grechka, V., and I. Tsvankin, 1998, Feasibility of nonhyperbolic moveout inversion in transversely isotropic media : Geophysics, **63**, 957–969, http://dx.doi.org/10.1190/1.1444407.

Helbig, K., and L. Thomsen, 2005, 75–plus years of anisotropy in exploration and reservoir seismics: A historical review of concepts and methods: Geophysics, **70**, no. 6, 9ND–23ND, http://dx.doi.org/10.1190/1.2122407.

Huang, T., S. Xu, and Y. Zhang, 2007, Anisotropy estimation for prestack depth migration-A tomographic approach: 77th Annual International Meeting, SEG, Expanded Abstracts, 124–128, http://dx.doi.org/10.1190/1.2792395.

Jiang, F., and H. Zhou, 2011, Traveltime inversion and error analysis for layered anisotropy: Journal of Applied Geophysics, **73**, 101–110.

Jiang, F., H. Zhou, Z. Zou, and H. Liu, 2009, 2D tomographic velocity model building in tilted transversely isotropic media: 79th Annual International Meeting, SEG, Expanded Abstracts, 4024–4028, http://dx.doi.org/10.1190/1.3255710.

Koren, Z., I. Ravve, G. Gonzalez, and D. Kosloff, 2008, Anisotropic local tomography: Geophysics, **73**, no. 5, VE75–VE92, http://dx.doi.org/10.1190/1.2953979.

Schleicher, K., J. Cramer, C. Gerrard, J. Jiao, S. Lin, A. Sosa, and C. Zhou, 2010, Model building for tilted transverse anisotropic depth migration of the Crystal Gulf of Mexico wide-azimuth survey: 72nd Conference and Exhibition, EAGE, Extended Abstracts, 39767.

Tsvankin, I., J. Gaiser, V. Grechka, M. Baan, and L. Thomsen, 2010, Seismic anisotropy in exploration and reservoir characterization: An overview: Geophysics, **75**, no. 5, 75A15–75A29, http://dx.doi.org/10.1190/1.3481775.

Tsvankin, I., and L. Thomsen, 1995, Inversion of reflection traveltimes for transverse isotropy: Geophysics, **60**, 1095–1107 http://dx.doi.org/10.1190/1.1443838.

Yuan, J., X. Ma, S. Lin, and D. Lowrey, 2006, P-wave tomographic velocity updating in 3D inhomogeneous VTI media: 76th Annual International Meeting, SEG, Expanded Abstracts, 3368–3372, http://dx.doi.org/10.1190/1.2370232.

Zhang, L., J. Zhang, and W. Zhang, 2012, Anisotropic effects on the near-surface seismic imaging: 82nd Annual International Meeting, SEG, Expanded Abstracts, http://dx.doi.org/10.1190/segam2012-0907.1.

Zhou, B., and S. A. Greenhalgh, 2005, Shortest path ray tracing for most general 2D/3D anisotropic media : Journal of Geophysics and Engineering, **2**, 54–63.

Zhou, H., D. Pham, S. Gray, and B. Wang, 2003, 3D tomographic velocity analysis in transversely isotropic media: 73rd Annual International Meeting, SEG, Expanded Abstracts, 650–653, http://dx.doi.org/10.1190/1.1818014.